AMERICAN JOURNAL OF RESEARCH IN MEDICAL SCIENCES, 2020
VOL 5, NO. 1, PAGE 1 – 5

RESEARCH ARTICLE

Open Access

A Novel Chiral Compound CCL441 Induces Mitotic Arrest and Apoptosis in Hepatoblastoma HepG2 Cells

Shuhan Guo[1], Yoshifumi Ohno[1], Ayumu Tsubosaka[1], Majid Vahed[1], Ruirong Yi[1], Xue Ma[1], Qisen Li[1], Kengo Saito[1], Shingo Nakamoto[1], Ryosuke Muroyama[1], Akiko Suganami[2,3], Yutaka Tamura[2,3], Akiko Tsuchida[3,4], Takayoshi Arai[3,4], and Hiroshi Shirasawa[1,*]

[1]Department of Molecular Virology, Graduate School of Medicine, Chiba University, 1-8-1 Inohana, Chuo-ku, Chiba 260-8670, Japan.
[2]Department of Bioinformatics, Graduate School of Medicine, Chiba University, 1-8-1 Inohana, Chuo-ku, Chiba 260-8670, Japan.
[3]Molecular Chirality Research Center, Chiba University, 1-33 Yayoi-chou, Inage-Ku, Chiba 263-8522, Japan.\
[4]Department of Chemistry, Graduate School of Sciences, Chiba University, 1-33 Yayoi-chou, Inage-Ku, Chiba 263-8522, Japan.

Introduction

Hepatoblastoma (HB) is the most common hepatic malignancy of childhood with frequent activation of Wnt/β-catenin signaling pathways [1]. The components of the Wnt/β-catenin pathway most involved in HB are the mutations located at exon 3 of CTNNB1 in a region of β-catenin important for its degradation via anaphase-promoting complex/cyclosome (APC/C) [2]. Familial adenomatous polyposis (FAP), which is caused by germline mutations at 5q22 in the APC/C gene, predispose to HB development with 750-7500 fold increase relative risk [2]. Due to the poor clinical prognosis, new therapeutic agents and targets for HB are sought.

Microtubule (MT)-targeting agents (MTAs) are a class of clinically successful anti-cancer drugs. MTs are found in mammalian cells and are involved in two different mitosis phases: interphase and division [3]. MTs consist of αβ-tubulin heterodimers that polymerize in a polarized way by a nucleation-elongation mechanism non-covalently adding dimers at the ends of MTs and forming hollow tubes. MTAs interfere with microtubule dynamics and arrest cancer cells in the G2/M phases; this can eventually induce apoptosis in cancer cells[4-6].

As MTAs disturb microtubule dynamics, these drugs often work by causing mitotic arrest that initiates apoptosis [7]. Mitosis is tightly regulated at the spindle assembly checkpoint (SAC) to ensure proper chromosomal segregation [8-10]. MTAs impair the dynamic balance of microtubule, thereby activate the SAC, which prevent cancer cells from entering anaphase through inhibiting the degradation of cyclin B1 by APC/C that controls the time to mitotic exit [10].

We screened a compound library for the development of therapeutic agents for HB and found a chiral compound CCL441, which shows specific toxicity to the HB cell line HepG2. Our study suggested that the CCL441 could be a microtubule-targeting agents (MTAs) which can be an anti-HB drug with a novel therapeutic modality.

Materials and Methods

Chemical compounds

The nitro group of 2-ethenyl-3-[2-nitro-1-phenylethyl]-1H-indole was reduced using a zinc nanopowder to give chiral tryptamine derivative, and the amine was tosylated to give CCL441, which was registered in the Chiba Chemical Library. The CCL441 was dissolved in dimethyl sulfoxide (DMSO, Wako) at 20 mM. The same volume of DMSO was used as a control. Phase-contrast microscopy (Nikon Eclipse TE2000-U; Nikon, Tokyo, Japan) was used to observe and photograph the morphology of cells.

ARTICLE HISTORY

Received June 30, 2020
Accepted July 30, 2020
Published August 05, 2020

KEYWORDS

Hepatoblastoma, HepG2, G2/M arrest, Apoptosis, Benzene-sulfonamide derivative, β-tubulin.

Cell culture

Human liver cancer cell line (HepG2), human epithelial cervical cancer cell line (HeLa), non-small-cell-lung cancer cell line (A549), normal human fibroblasts (TIG-1-20), and monkey kidney cell line (Vero) were maintained in Dulbecco's Modified Eagles' medium (DMEM) supplemented with 10% (v/v) fetal bovine serum (FBS) at 37 ºC with 5 % CO_2 in a humidified atmosphere.

Flowcytometry

Cells were cultured in 6 cm dish (3×10^5 cells) for 24 h, and then cells were treated with ten µmol/L of CCL441 or DMSO for further 24 h. Cells were collected and washed twice with phosphate-buffered saline (PBS). Next, cells were treated with reagents from the CycleTEST™ PLUS DNA Reagent Kit (Becton Dickinson and Company, Franklin Lakes, NJ, USA) and analyzed on a BD Accuri™ C6 Flow Cytometer (Becton Dickinson and Company, Franklin Lakes, NJ, USA) equipped with FACScan's fluorescence 2 (FL2) detector. The collected data were analyzed using FlowJo 7.6.5 (TreeStar Company, San Carlos, CA, USA).

Contact Shirasawa H ✉ Department of Molecular Virology, Graduate School of Medicine, Chiba University, 1-8-1 Inohana, Chuo-ku, Chiba 260-8670, Japan, Tel: +81-43-226-2044; Fax: +81-43-226-2045

Western blotting

Cells were seeded at 6 cm dish (3×10^5 cells) for 24 h, and then cells were treated with ten µmol/L of CCL441 or DMSO for further 24 h. Cells were collected and washed twice with PBS. An equal number of treated and untreated cells were resuspended in an equal volume of M-PER® Mammalian Protein Extraction Reagent (Thermo Fisher Scientific, Waltham, MA, USA) with a cocktail of protease inhibitor (Sigma-Aldrich, Steinheim, Germany) and mixed gently for 10 minutes. Lysates were centrifuged at 14,000 × *g* for 15 min. Equal volumes of extracted protein were loaded onto SDS-polyacrylamide gels (Atto Corporation, Tokyo, Japan), transferred onto PVDF membranes (Trans-Blot Turbo™ Transfer Pack; BIO-RAD, Hercules, CA, USA). After transfer, the PVDF membranes were washed with PBS containing 0.1 % of Tween 20 and incubated with the above-mentioned primary antibodies overnight at 4 °C. PVDF membranes were rewashed and incubated with a 1:2000 dilution of second antibodies for 2 h at room temperature. Proteins were detected by using ECL plus kit (BIO-RAD, Hercules, CA, USA), and protein bands were detected with ECL Western Blotting Detection Reagents (GE Healthcare, Tokyo, Japan).

ATP assays

Cell viability was determined by ATP assays using the Cell Titer-Glo® Luminescent Cell Viability Assay kit (Promega, Madison, WI, USA) to assess cell viabilities according to manufacturer's instruction with a microplate reader (Wallac 1420 ARVOsx Multilabel Counter; PerkinElmer, Chiba, Japan).

Caspase-3/7 assays

HepG2 cells were plated in 96-well plate at a density of 5.0×10^4 cells per well for 24h. The cells were then treated with ten µM of CCL441 or DMSO for 24 h. Caspase-3 and 7 activities were measured using the Caspase-Glo 3/7 Assay (Promega, Japan).

Molecular docking simulations

The protein geometry of αβ-tubulin was obtained from the cryo-electron microscopy structure of the protein available in the RCSB protein data bank with the accession code 5syf [11]. Before proceeding with the analysis, all solvent molecules and compounds were removed from the structure. The α- and β-tubulin structures in the αβ-tubulin complex were divided into two separate files for individual docking analyses. The 3-D chemical structures of colchicine, taxol, and CCL441 were designed using the software Avogadro (version 1.1.1) [12]; the structures were optimized in Gaussian 16 (Gaussian Inc.) at the B3LYP/6-31G (d, p) theoretical level [13]. The software AutoDock 4.2 [14] was utilized for molecular docking simulations. Structure files for proteins and ligands were made in the PDBQT format using default charges; furthermore, nonpolar hydrogen atoms were conjoined using AutoDockTools (version 1.5.6). A grid box comprised of dimensions 76 Å × 76 Å × 76 Å XYZ was centered on the tubulin structure. A pre-calculated binding affinity value for each ligand's atom type was prepared using Autogrid. Rigid docking was accomplished using a Lamarckian genetic algorithm parameter [14]. All other parameters in the AutoDock 4.2 software were default settings. The best pose for docking was selected based on the lowest values of binding energies obtained. The free binding energies (FBE) and van der Waals (VDW) interactions were computed using a linear regression model built in the AutoDock. The hydrogen bond (H-bond) occupancy for visualization of docked conformations was obtained using PyMOL[15]. The root means square deviation (RMSD) values for ligands were calculated using PyMOL. The structure of β-tubulin with helix axes was generated using the molecular modeling software Chimera [16].

Statistical analysis

Statistical analyses were performed using Statcel4, version 4 (OMS, Tokyo, Japan). All values were expressed as mean ± standard error (SE) from three biologically independent determinations. Values of $P < 0.05$ were considered statistically significant.

Results

Screening of anti-hepatoblastoma compounds in Chiba Chemical Library

We screened a chemical compound library (CCL) for anticancer compounds [16] that could show selective cytotoxicity against hepatoblastoma cell line HepG2. A novel compound CCL441 (Figure 1A), a benzene-sulfonamide derivative [17], was identified to exhibit cytotoxicity against only HepG2.

Cytotoxic effect of CCL441 against HepG2 cells

Cell viability assays for CCL441-treated cancer cells (hepatoblastoma cell line HepG2, cervical cancer cell line HeLa, and non-small-cell-lung cancer cell line A-549) and normal human fibroblasts TIG-1-20, and monkey kidney cell line Vero showed that 10 µM of CCL441 exhibited cytotoxicity only against HepG2 (Figure1B) with a morphological changes of round cells (Figure 1C). CCL441 exhibited cytotoxicity against HepG2 in a dose-dependent, and time-dependent manner (Figure 1D). All further experiments were performed at a concentration of 10 µM. To confirm the cytotoxic activity of the CCL441, we examined the activity of caspase 3/7 in HepG2 cells treated with the compound using the Caspase-Glo 3/7 Assay kit (Promega, Japan). The caspase 3/7 were activated in HepG2 cells treated with ten µM of CCL441, indicating that the CCL441 caused apoptosis in HepG2 cells (Figure 1E).

Flow cytometry analyses of HepG2 cells treated with CCL441

To assess the effects of CCL441 on the cell cycle, we treated HepG2 cells with ten µM of CCL441 for 24 h, then analyzed by flow cytometry (Figure 2A). The cells in the G2/M phases significantly increased, and the cells in the G1/S phases decreased in HepG2 cells treated with CCL441, suggesting the CCL441 caused G2/M arrest (Figure 2B). To confirm the arrest of HepG2 cells treated with CCL441 in the G2/M phase, we examined the expression of p-histone H3 and Cyclin B1. The histone H3 is phosphorylated during mitosis [18] , and the cyclin B is essential for driving mitotic events, and the degradation of cyclin B is a prerequisite event at the metaphase for the exit of mitosis [10]. As shown in Figure 2C, the expression levels of p-histone H3 in CCL441-treated HepG2 cells elevated remarkably after 24 hrs treatment of CCL441, and the Cyclin B1 in the HepG2 cells treated with CCL441 were higher than those DMSO-treated HepG2 cells, suggesting the CCL441 may cause the accumulation of the cells at the M phase before the metaphase.

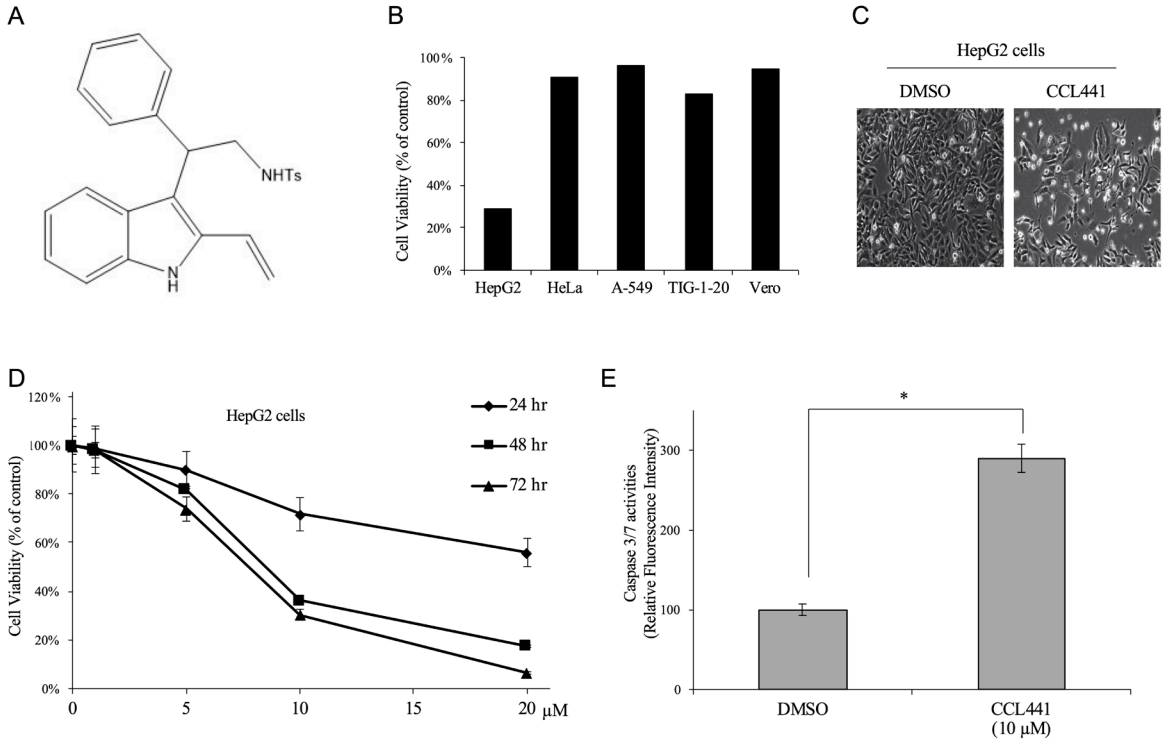

Figure 1 Cytotoxic effects of CCL441 on HepG2 cells. (A) Chemical structure of CCL441, a chiral tosylated tryptamine derivative. (B) Cell viabilities of CCL441-treated HepG2, HeLa, A-549, TIG-1-20, and Vero cells at a concentration of 10 μM for 72 h. Cell viabilities are represented as percentage of the vehicle control (10μM of DMSO). (C) Effect of CCL441 on the morphology of HepG2 cells. Cells were treated with 10 μM of CCL441 or DMSO for 72h. (D) Cytotoxicities of CCL441 against HepG2. HepG2 cells were treated with increasing concentrations of CCL441 for 24, 48, and 72 h. Data are shown as mean ± SE, and cell viabilities are represented as percentage of the control group for three independent experiments. (E) Caspase 3/7 activities in HepG2 cells treated with 10 μM of DMSO or CCL441 for 24 h. Data are shown as mean ± SE for three independent experiments. *P<0.005 (Mann-Whitney U-test)

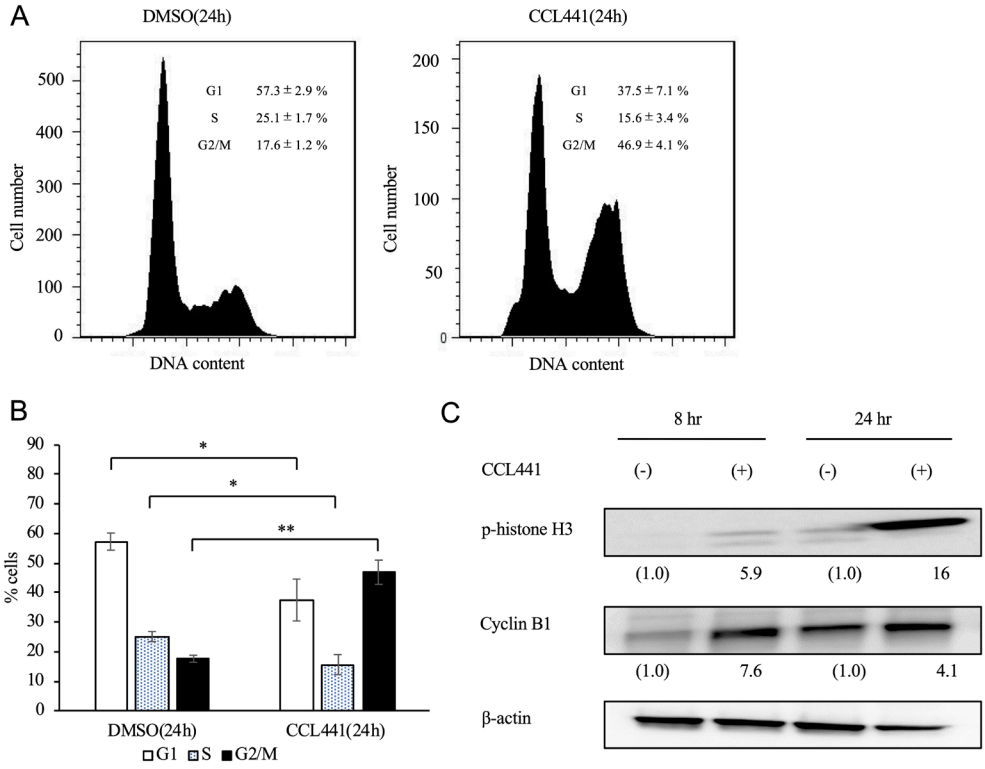

Figure 2: Effects of CCL441 on cell cycle progression. (A) Representative histograms of the flow cytometry data on cell cycle progression in HepG2 cells following 24 h of treatment with 10 μM of DMSO or CCL441. (B) The proportions of HepG2 cells in G1, S, and G2/M phases following 24 h of treatment with DMSO or CCL441. Data are represented as mean ± SE of three independent experiments. *P<0.05, **P<0.001 (Mann-Whitney U-test).

Docking study of CCL441 with β-tubulin

Since CCL441 was supposed to have an activity of disturbing mitosis, the possibility of CCL441 interaction with tubulin was assessed by a docking study. The best 3-D formations of CCL441 were generated using Gaussian16 for the docking study (Figure 3A, CCL441-i, CCL441-ii, and CCL441-iii). The ligand-protein docking showed different free binding energies for α- and β-tubulin with CCL441. Since all binding energies were significantly lower for β-tubulin/CCL441 complexes, β-tubulin was used for further ligand-binding analyses. The colchicine and taxol were docked with the β-tubulin as controls.

CCL441 exhibited high binding affinities to the taxol binding domain (TBD) and colchicine binding domain (CBD) (Figure 3B). As shown in Table 1, the lowest free binding energy (FBE) score at TBD was -4.96 Kcal of CCL441-iii, which was compatible with that of taxol, and the lowest FBE at CBD was -3.98 Kcal of CCL441-i. The lowest-energy superposition of CCL441-i, CCL441-ii, and CCL441-iii docked with β-tubulin were shown in Figure 3C. The lowest energy of VDW interaction was that of CCL441-iii at TBD. The lowest RMSD value, 0.96 was found for CCL441-ii at TBD, and one hydrogen-bond interaction of CCL441-i at CBT was formed for residue N258 (Figure 4A), one hydrogen-bond interaction of CCl441-ii at TBD was formed for residue P274 (Figure 4B), and none for CCL441-iii (Figure 4C). Notably, the values of VDW interactions, VDV, and RMSD were not closely correlated with the FBE of the compounds.

Discussion

In this study, we showed that the CCL441 induced cell cycle arrest in the M phase followed by apoptosis in hepatoblastoma cell line HepG2. Interestingly, CCL441 exhibited no cytotoxicity to a cervical cancer cell line, HeLa, a lung cancer cell line, A-549, normal human fibroblasts, TIG-1-20, and normal monkey kidney cell line, Vero. Although the precise mechanism of the specific cytotoxicity of CCL441 against hepatoblastoma cell line HepG2 remains unknown, our study suggested that the HepG2-specific compromised response to a possible MTA, CCL441, could be involved in the mitotic apoptosis.

The docking study showed that CCL441 could bind to β-tubulin at both the colchicine-binding and taxol-binding domain. The high affinity of CCL441 to both binding domains might be due to the chirality of the CCL441. The colchicine and taxol bind to a different site of β-tubulin, and have different effects on tubulin dynamics; the colchicine inhibits the formation of the microtubule, and the taxol inhibits the disassembly of the microtubules [3]. Since known MTAs binds to a single domain of the β-tubulin, the effect of CCL441 on the dynamics of the microtubule should be different from other MTAs.

Flow cytometry analyses showed that HepG2 cells treated with CCL441 accumulated at the G2/M phase. Besides, elevated expression of p-histone H3 and accumulation and elevated expression of cyclin B1 suggested CCL441 inhibited the exit from the M phase. For the exit from the mitosis, the APC-mediated degradation of cyclin B1 is necessary. Since APC is also involved in the Wnt/β-catenin pathways that are compromised in HepG2 cells, the regulation of mitotic exit in HepG2 might be vulnerable to the mitotic stress, such as MTA-induced mitotic arrest. Therefore, the specific cytotoxicity of CCL441 against HepG2 cells might be due to the CCL441-caused mitotic stress.

HepG2 is a hepatoblastoma (HB)-derived cell line with activation of mutated β-catenin. The mutations located at exon 3 of CTNNB1 in a region of β-catenin important for its

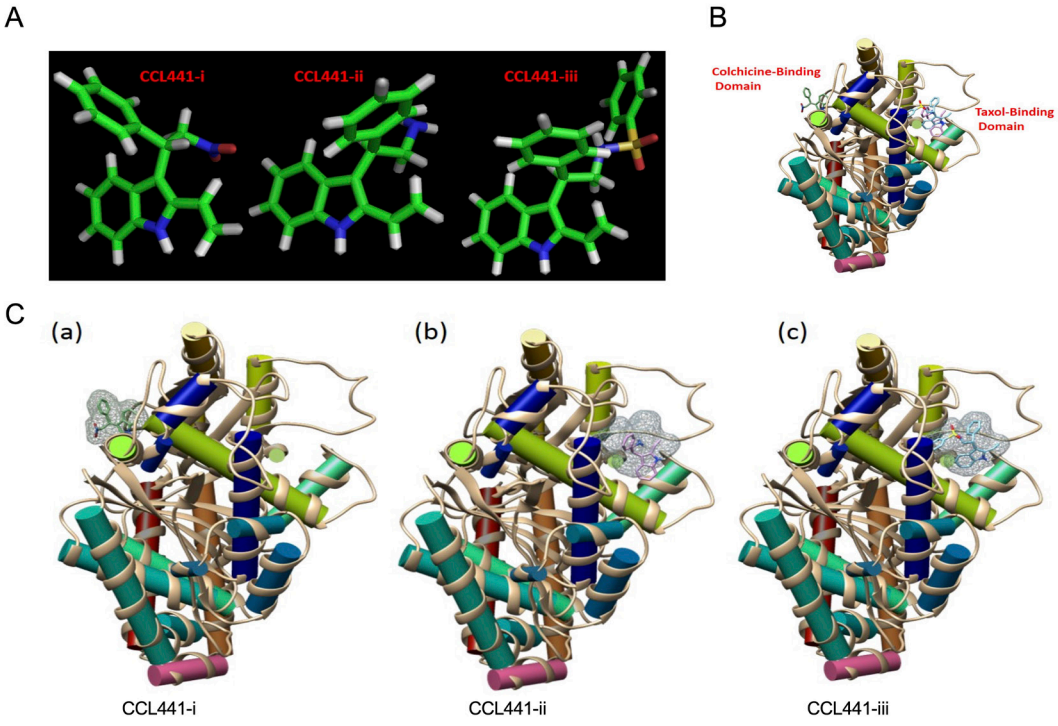

Figure 3: Docking analyses of the interactions between CCL441 and β-tubulin. (A) Structures of optimized geometries of CCL441-enantiomers, CCL441-i, CCL441-ii, and CCL441-iii. (B) Atomic geometries of CCL441-bound β-tubulin at colchicine-binding domain and taxol-binding domain. (C) Atomic geometries of ligand-bound β-tubulin with lowest binding energy for CCL441-enantiomers. The interactions of CCL441-i at colchicine-binding domain (a), CCL441-ii at taxol-binding domain (b), and CCL441-iii at taxol binding domain.

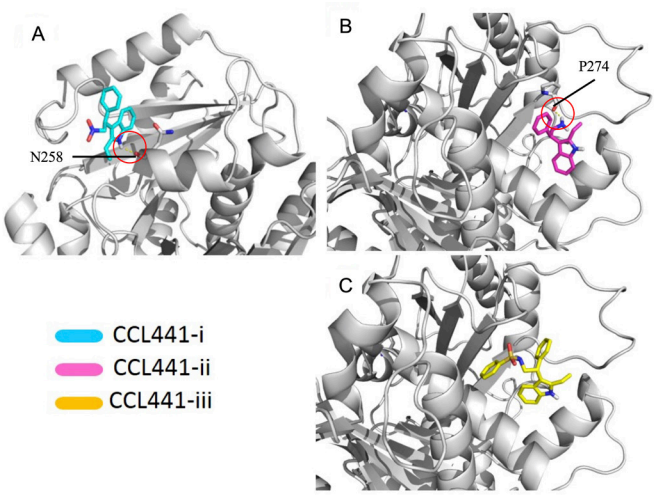

Figure 4: Hydrogen bonds formed between CCL441-enantiomers and β-tubulin. Hydrogen bonds with lower energy were formed between residue N258 and CCL441-i (A), P274 and CCL441-ii. No hydrogen bonds were formed between β-tubulin and CCL441-iii (C).

Table 1. Docking scores of CCL441, colchicine, and taxol with β-tubulin.

Compound	CCL441-i	CCL441-ii	CCL441-iii	colchicine	taxol
binding domain	CBD[a]	TBD[b]	TBD	CBD	TBD
FBE*	-3.98	-3.80	-4.96	-4.24	-4.81
VDW**	-5.46	-5.26	-7.10	-5.63	-9.01
RMSD***	1.65	0.96	2.80	0.36	2.18
H-bond****	1	1	0	4	2

*Free Binding Energy
**Van Der Waals
***Root-Mean-Square Deviation
****Hydrogen bond
[a] colchicine binding domain.
[b] taxol binding domain.

degradation by the proteasome containing APC [19]. The fact that the familial adenomatous polyposis (FAP), which is caused by germline mutations at 5q22 in the APC gene, predisposes to HB development [19] suggests that APC in HB with mutated β-catenin may be disturbed and vulnerable to stress caused by MTAs.

Although MTAs have not been described as an anti-HB drug, the CCL441 can be a unique MTA as it can bind both to the colchicine domain and the taxol domain. Our study suggested that the CCL441 may be a microtubule-targeting agents with a new therapeutic modality to hepatoblastoma.

Funding

This work was supported by JSPS KAKENHI Grant Number JP26430155.

References

[1] Sha YL, Liu S, Yan WW, Dong B. Wnt/β-catenin signaling as a useful therapeutic target in hepatoblastoma. Biosci Rep. 2019; 39: 53–10.

[2] Morcrette G, Hirsch TZ, Badour E, Pilet J, Caruso S, Calderaro J, et al. APC germline hepatoblastomas demonstrate cisplatin-induced intratumor tertiary lymphoid structures. Oncoimmunology. Taylor & Francis. 2019; 8: e1583547.

[3] Mukhtar E, Adhami VM, Mukhtar H. Targeting Microtubules by Natural Agents for Cancer Therapy. Mol. Cancer Ther. 2014; 13: 275–84.

[4] Bhalla KN. Microtubule-targeted anticancer agents and apoptosis. Oncogene. Nature Publishing Group; 2003; 22: 9075–9086.

[5] Jordan MA, Wilson L. Microtubules as a target for anticancer drugs. Nat Rev Cancer. Nature Publishing Group; 2004; 4: 253–265.

[6] Rohena CC, Mooberry SL. Recent progress with microtubule stabilizers: new compounds, binding modes and cellular activities. Nat Prod Rep. The Royal Society of Chemistry; 2014; 31: 335–355.

[7] Haschka MD, Soratroi C, Kirschnek S, Häcker G, Hilbe R, Geley S, et al. The NOXA-MCL1-BIM axis defines lifespan on extended mitotic arrest. Nat Commun. Nature Publishing Group; 2015; 6: 6891.

[8] Liu X, Chen Y, Li Y, Petersen RB, Huang K. Targeting mitosis exit_ A brake for cancer cell proliferation. BBA - Reviews on Cancer. Elsevier; 2019; 1871: 179–91.

[9] Hayashi Y, Shino Y, Saito K, Tanzawa H, Shirasawa H. c-Jun-mediated repression and transactivation of fibronectin. Mol Med Report. 2008; 1: 99–103.

[10] Musacchio A. The Molecular Biology of Spindle Assembly Checkpoint Signaling Dynamics. Curr. Biol. 2015; 25: R1002–18.

[11] Kellogg EH, Hejab NMA, Howes S, Northcote P, Miller JH, Díaz JF, et al. Insights into the Distinct Mechanisms of Action of Taxane and Non-Taxane Microtubule Stabilizers from Cryo-EM Structures. Journal of Molecular Biology. 2017; 429: 633–646.

[12] Hanwell MD, Curtis DE, Lonie DC, Vandermeersch T, Zurek E, Hutchison GR. Avogadro: an advanced semantic chemical editor, visualization, and analysis platform. J Cheminform. Nature Publishing Group; 2012; 4: 17.

[13] Becke AD. Density-functional thermochemistry. III. The role of exact exchange. The Journal of Chemical Physics. American Institute of Physics; 1998; 98: 5648–5652.

[14] Morris GM, Huey R, Lindstrom W, Sanner MF, Belew RK, Goodsell DS, et al. AutoDock4 and AutoDockTools4: Automated docking with selective receptor flexibility. Journal of Computational Chemistry. Wiley-Blackwell; 2009; 30: 2785–2791.

[15] Eisenberg D, Schwarz E, Komaromy M, Wall R. Analysis of membrane and surface protein sequences with the hydrophobic moment plot. Journal of Molecular Biology. 1984; 179: 125–142.

[16] Chen W. Novel Chiral Chalcone Analogs that Induce M Phase Arrest and Apoptosis in HeLa Cells. Medicinal Chemistry. 2019; 9: 74–82.

[17] Arai T, Tsuchida A, Miyazaki T, Awata A. Catalytic Asymmetric Synthesis of Chiral 2-Vinylindole Scaffolds by Friedel-Crafts Reaction. Org. Lett. 2017; 19: 758–761.

[18] Crosio C, Fimia GM, Loury R, Kimura M, Okano Y, Zhou HY, et al. Mitotic phosphorylation of histone H3: Spatio-temporal regulation by mammalian aurora kinases. Mol. Cell. Biol. 2002; 22: 874–885.

[19] Laflamme G, Sim S, Leary A, Pascariu M, Vogel J, D'Amours D. Interphase Microtubules Safeguard Mitotic Progression by Suppressing an Aurora B-Dependent Arrest Induced by DNA Replication Stress. Cell Reports. 2019; 26: 2875–2889.e3.